

Primary Tumor Hypoxia Recruits CD11b⁺/Ly6C^{med}/Ly6G⁺ Immune Suppressor Cells and Compromises NK Cell Cytotoxicity in the Premetastatic Niche

Jaclyn Sceneay^{1,4}, Melvyn T. Chow^{2,4}, Anna Chen^{1,4}, Heloise M. Halse², Christina S.F. Wong¹, Daniel M. Andrews², Erica K. Sloan⁷, Belinda S. Parker^{3,4,5}, David D. Bowtell^{1,4,5,6}, Mark J. Smyth^{2,4,5,6}, and Andreas Möller^{1,4,5,6}

Abstract

Hypoxia within a tumor acts as a strong selective pressure that promotes angiogenesis, invasion, and metastatic spread. In this study, we used immune competent bone marrow chimeric mice and syngeneic orthotopic mammary cancer models to show that hypoxia in the primary tumor promotes premetastatic niche formation in secondary organs. Injection of mice with cell-free conditioned medium derived from hypoxic mammary tumor cells resulted in increased bone marrow–derived cell infiltration into the lung in the absence of a primary tumor and led to increased metastatic burden in mammary and melanoma experimental metastasis models. By characterizing the composition of infiltrating bone marrow–derived cells, we identified CD11b⁺/Ly6C^{med}/Ly6G⁺ myeloid and CD3⁻/NK1.1⁺ immune cell lineages as key constituents of the premetastatic niche. Furthermore, the cytotoxicity of natural killer (NK) cells was significantly decreased, resulting in a reduced antitumor response that allowed metastasis formation in secondary organs to a similar extent as ablation of NK cells. In contrast, metastatic burden was decreased when active NK cells were present in premetastatic lungs. Together, our findings suggest that primary tumor hypoxia provides cytokines and growth factors capable of creating a premetastatic niche through recruitment of CD11b⁺/Ly6C^{med}/Ly6G⁺ myeloid cells and a reduction in the cytotoxic effector functions of NK cell populations. *Cancer Res*; 72(16); 3906–11. ©2012 AACR.

Introduction

Hypoxia is a common feature and poor prognostic marker in several solid cancers (1). Cells respond to hypoxia through stabilization of the Hypoxia-inducible factor (Hif) transcription factor, resulting in the expression of genes involved in angiogenesis, invasion, and metastasis (1).

Hypoxia controls the composition of the tumor microenvironment and the invasive and metastatic capacity of various cancers (2). Factors capable of inducing bone marrow–derived

cell (BMDC) mobilization and recruitment to the tumor microenvironment include Hif targets VEGF, angiopoietin-1, PIGF, PDGF-B, and SDF1 α (3). Emerging evidence suggests primary tumor hypoxia and BMDCs drive premetastatic niche development in distant tissues, making them permissive for metastatic spread (4, 5).

Premetastatic niche formation was first attributed to tumor-derived VEGF- and PIGF-induced secretion of fibronectin from fibroblasts, promoting adhesion of VEGFR1⁺ hematopoietic progenitor cells (6). Additional studies reported alternate mechanisms for premetastatic niche formation involving TNF α , TGF β , lysyl-oxidase (LOX), MMP2, MMP9, CXCR4, and SDF1 α among others (7). Most of these are direct or indirect Hif targets and generally important in the metastatic process (1). Although secretion of these factors by the primary tumor increases BMDCs in premetastatic organs, in-depth characterization of the responsive BMDCs lineages is lacking.

Here we report that conditioned medium containing monocyte chemoattractant protein-1 (MCP-1/CCL2), derived from hypoxic mammary tumor cells, can induce premetastatic niche formation in the lungs of immune-competent animals. Furthermore, we define lung infiltrating, bone marrow–derived CD11b⁺/Ly6C^{med}/Ly6G⁺ myeloid cells and natural killer (NK) cells with reduced antitumor responses, which form a premetastatic niche conducive to increased metastatic burden independent of tumor type.

Authors' Affiliations: ¹Cancer Genomics and Genetics Laboratory, ²Cancer Immunology Program, and ³Metastasis Research Group, Peter MacCallum Cancer Centre, St. Andrews Place, East Melbourne; ⁴Department of Pathology, ⁵Sir Peter MacCallum Department of Oncology, ⁶Department of Biochemistry, The University of Melbourne; and ⁷Monash Institute of Pharmaceutical Sciences, Monash University, Parkville, Victoria, Australia

Note: Supplementary data for this article are available at Cancer Research Online (<http://cancerres.aacrjournals.org/>).

M.J. Smyth and A. Möller contributed equally to this work.

Corresponding Authors: Andreas Möller and Mark Smyth, Peter MacCallum Cancer Centre, St. Andrews Place, East Melbourne, Victoria 3002, Australia. Phone: 613-9656-1423; Fax: 613-9656-1411; E-mail: andreas.moeller@petermac.org and mark.smyth@petermac.org.

doi: 10.1158/0008-5472.CAN-11-3873

©2012 American Association for Cancer Research.

Materials and Methods

Mice

Female C57Bl/6 mice were used at 8 to 14 weeks and purchased from the Walter and Eliza Hall Institute (Melbourne). C57Bl/6 NZeg-enhanced GFP (eGFP) mice were used as bone marrow donors for chimeras generated as previously described (6, 8). C57Bl/6 Rag2^{-/-}c.γ^{-/-} mice were bred and maintained at the Peter MacCallum Cancer Centre. All animal procedures were approved by the Peter MacCallum Cancer Centre Animal Experimentation Ethics Committee.

Cell lines and conditioned media assays

The EO771 and PyMT mammary carcinoma and B16F10 melanoma cell lines were maintained as previously described (9, 10) and infected with the pMSCV-Cherry/Luciferase lentiviral vector for sorting by flow cytometry. Conditioned media was generated by filtering serum-free, phenol red-free low glucose Dulbecco's Modified Eagles Medium (Invitrogen) cultured on cells for 10 hours under normoxic (20% O₂) or hypoxic conditions (2% O₂; ref. 6). Conditioned media (300 μL) was injected intraperitoneally daily for 7 days and lungs harvested the following day. For experimental metastasis models, mice were injected with 2 × 10⁵ tumor cells intravenously on day 7, as detailed in Supplementary Methods.

Cytokine/angiogenesis arrays

Secreted factors in conditioned media were detected using Proteome Profiler array kits (R&D Systems), according to the manufacturers' instructions.

Flow cytometry

Flow cytometry was carried out on a single-cell suspension of whole lung tissue (10). Antibody details listed in Supplementary Methods.

⁵¹Cr release cytotoxicity assay

CD3⁻/NK1.1⁺ cells were sorted using fluorescence-activated cell sorting from whole lung as above. ⁵¹Cr-labeled YAC-1 target cells were used in a standard 4-hour NK cell cytotoxicity assay (10).

Immunofluorescence

eGFP visualization and immunofluorescence was carried out on ornithine carbamyl transferase-inflated lungs. Sections were stained with CD11b (BD Pharmingen) and images taken on a BX-51 microscope (Olympus).

Statistical analyses

Results are expressed as mean ± SEM and analyzed by 2-tailed Mann-Whitney nonparametric *t* tests, *P* values less than 0.05 were considered significant (***, *P* < 0.0001; **, *P* < 0.01; *, *P* < 0.05).

Results and Discussion

Tumor hypoxia causes BMDC accumulation in lungs

To examine the impact of factors produced by hypoxic tumor cells on BMDC recruitment to certain organs, eGFP⁺

bone marrow chimeric mice were injected with normoxic (20% O₂) or hypoxic (2% O₂) cell-free conditioned medium (NCM and HCM, respectively) derived from PyMT-WT or Siah2^{-/-} mammary tumor cell lines. Siah2^{-/-} cells lack a functional hypoxic response due to failure to stabilize Hif-1α under hypoxic conditions (9). HCM-treated mice showed a significant increase in eGFP⁺ BMDCs in lungs, compared with mice injected with either NCM, Siah2^{-/-} NCM, or Siah2^{-/-} HCM (Fig. 1A). Clusters of eGFP⁺/CD11b⁺ cells were also more frequently observed at terminal bronchioles of the lung in WT HCM-treated mice (Fig. 1B). Therefore, factors secreted from hypoxic mammary tumor cells alone, increase the accumulation of CD11b⁺ BMDCs in the lung.

A strong stabilization of Hif-1α protein was observed in both PyMT-WT and EO771 cells after 2 and 10 hours hypoxia exposure compared with normoxia (Supplementary Fig. S1A). In contrast, Hif-2α protein was only marginally stabilized under hypoxia (Supplementary Fig. S1A). This suggested that formation of the premetastatic niche is driven by Hif-1α signaling in hypoxic tumor cells, although a contribution from exclusively Hif-2α-regulated genes cannot be excluded (11).

Factors secreted from hypoxic tumor cells promote metastasis formation

To determine whether BMDC recruitment creates a premetastatic niche supportive of tumor cell colonization and metastatic outgrowth, we injected NCM or HCM derived from PyMT-WT and EO771 mammary tumor cells, followed immediately by intravenous injection of Cherry-labeled PyMT-WT or EO771 tumor cells (Supplementary Fig. S1B). Naive mice intravenously injected with Cherry-labeled tumor cells alone (IV only group), without exposure to conditioned medium, served as positive controls. HCM treatment increased metastatic colonization by PyMT-WT or EO771 Cherry-positive tumor cells compared with NCM (Fig. 1C and D). These data showed that pretreatment with HCM supports the colonization and outgrowth of a greater number of metastatic tumor cells in preconditioned lungs by modulating the microenvironment of distant tissues.

We next defined whether the premetastatic lung environment created by mammary tumor cell-derived HCM also supported metastasis formation of other tumor types. Mice pretreated with NCM or HCM from PyMT-WT tumor cells were intravenously injected with B16F10 melanoma cells. We observed a significant increase in metastatic foci in lungs of HCM compared with NCM-treated mice (Fig. 2A; Supplementary Fig. S2A). Hence, HCM derived from mammary tumor cells modifies lungs to be generally receptive to circulating tumor cells, suggestive of a premetastatic niche with reduced anti-tumor responses.

To identify factors contributing to premetastatic niche formation, proteins secreted from hypoxic PyMT-WT and EO771 cells were assessed. HCM contained increased MCP-1 (CCL2), G-CSF, TNF-α, VEGF, TIMP-1, and MMP-9 (Fig. 2B and C; Supplementary Fig. S2B). Several of these factors have been separately reported in premetastatic niche formation (highlighted in Supplementary Fig. S2B; refs. 7, 12, 13), and thus hypoxia within the primary tumor may be the unifying

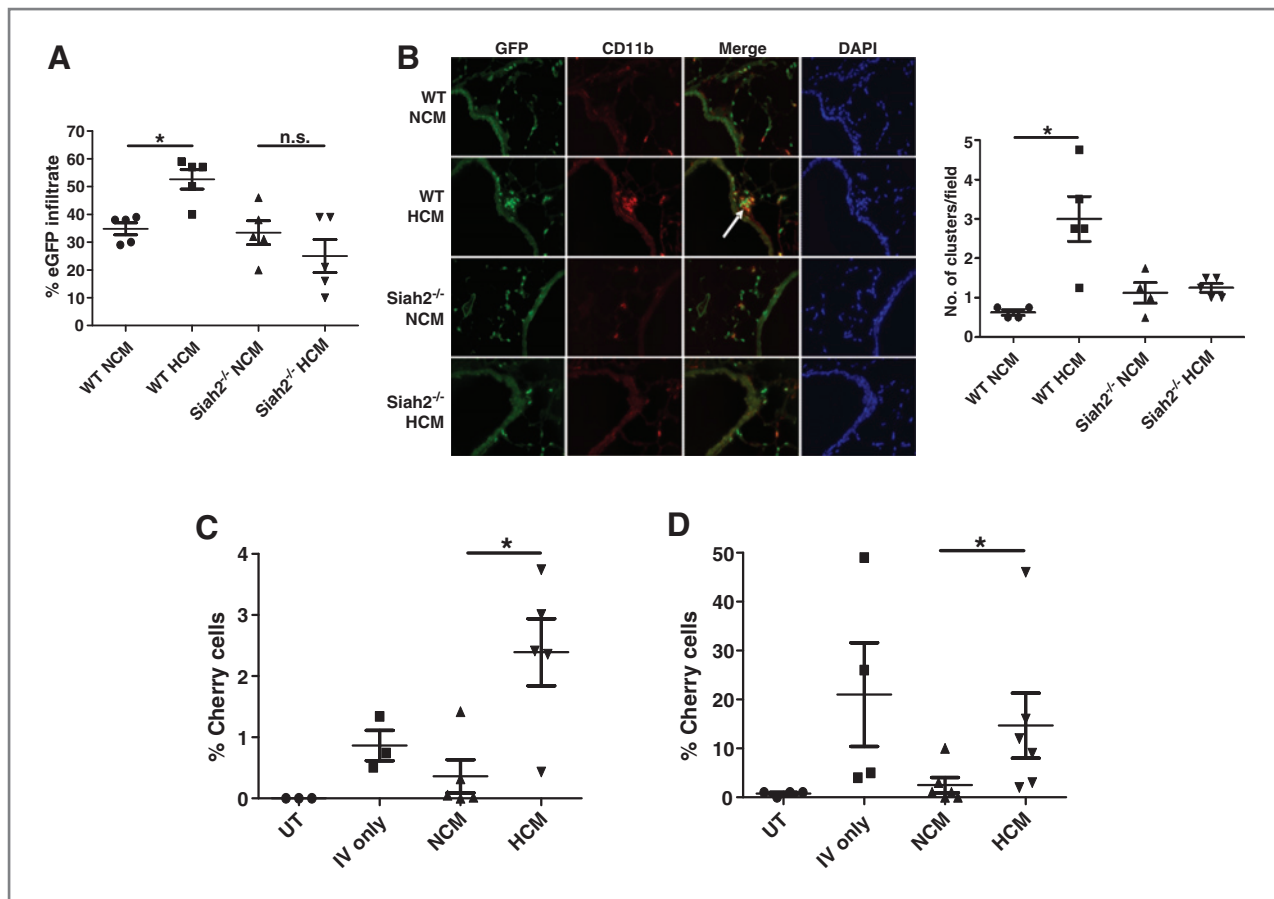


Figure 1. HCM induces eGFP⁺/CD11b⁺ BMDC infiltration into lungs. **A**, percentage eGFP-positive BMDCs in the lungs of eGFP bone marrow chimeric mice injected with PyMT-WT or Siah2^{-/-} NCM/HCM ($n = 5$ per group). **B**, lung sections from **A** costained with CD11b and 4', 6-diamidino-2-phenylindole (DAPI) identify clusters of eGFP⁺/CD11b⁺ cells (indicated by arrowhead). Five images per section (4–5 mice/group) were counted and summarized graphically. **C** and **D**, Cherry-positive tumor cell burden in lungs analyzed by flow cytometry in PyMT-WT (**C**) and EO771 (**D**) models at 2 and 4 weeks respectively after injection [$n = 3$ UT (untreated)/IV only groups; $n = 5$ NCM/HCM]. Mean percentage \pm SEM.

process that drives premetastatic niche formation during tumorigenesis. MCP-1 is a member of the CC chemokine β -subfamily known to regulate the recruitment of inflammatory cells into tissues during inflammation and cancer (14) and is increased in both PyMT-WT and EO771 HCM. Neutralization of MCP-1 in PyMT-WT HCM using a MCP-1 antibody decreased metastatic burden compared with HCM treatment alone (Fig. 2D). In contrast, MCP-1 neutralization in NCM did not alter metastatic burden compared with NCM treatment alone (Fig. 2D). Thus increased metastatic burden observed after HCM treatment (Fig. 1C and D) can, in part, be attributed to increased MCP-1 present in hypoxic tumor cell conditioned medium.

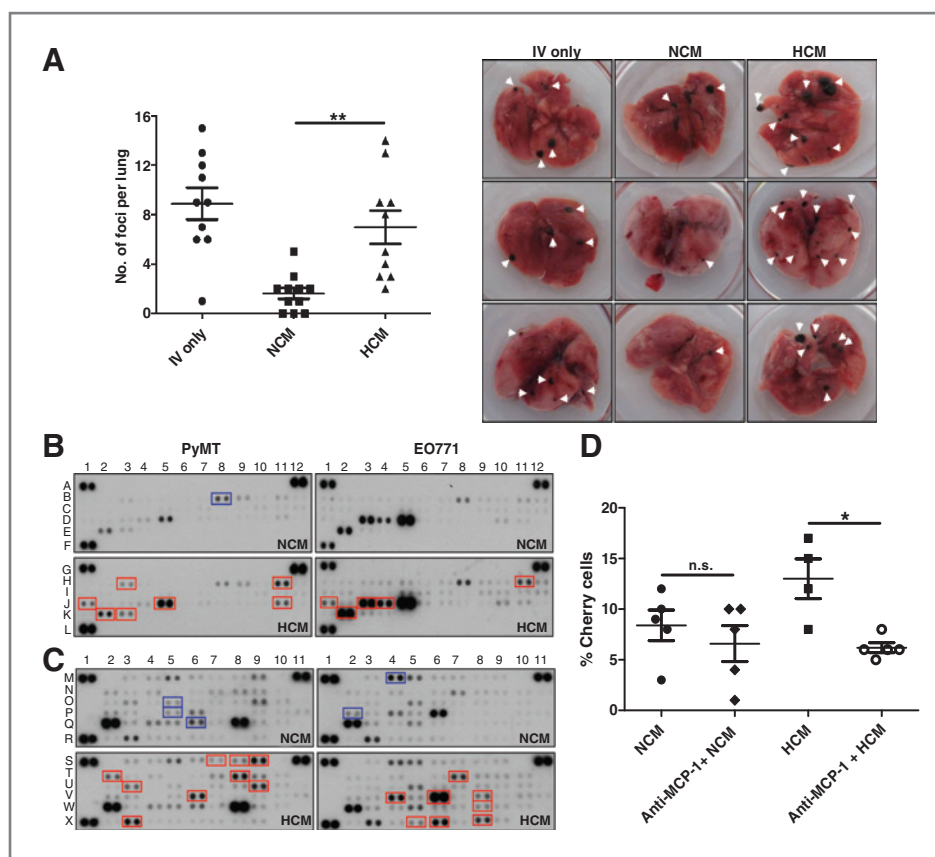
Recruitment of CD11b⁺/Ly6C^{med}/Ly6G⁺ BMDCs to the premetastatic niche

We hypothesized that the prometastatic effects of HCM treatment would be determined by the type and function of immune cells present. CD11b⁺/Gr-1⁺ myeloid cells have been previously described in the premetastatic niche (5, 7, 12, 13, 15). This heterogeneous group of cells includes precursors of macrophages, granulocytes, dendritic cells, and myeloid cells

at various stages of differentiation (16). Examination of bone marrow-derived myeloid cells for Ly6G⁺ and Ly6C⁺ subtypes (both recognized by the Gr-1 antibody) revealed that only CD11b⁺/Ly6C⁺ cells were significantly increased in the lungs of HCM-treated mice (Fig. 3A). Two subpopulations of CD11b⁺/Ly6C⁺ cells with different levels of Ly6C expression (denoted Ly6C^{med} and Ly6C^{high}) were identified (Fig. 3B). Only the CD11b⁺/Ly6C^{med} cells (Fig. 3B middle panel), but not CD11b⁺/Ly6C^{high} cells (Fig. 3B right panel), were significantly increased in HCM-treated mice. Ly6G was coexpressed on more than 75% of CD11b⁺/Ly6C^{med} cells in both groups compared with 30% of CD11b⁺/Ly6C^{high} cells (Fig. 3C). This defines 2 distinct subsets of Ly6C⁺ myeloid cells, CD11b⁺/Ly6C^{high}/Ly6G⁻ and CD11b⁺/Ly6C^{med}/Ly6G⁺, with only the latter increased in premetastatic organs after HCM treatment.

The CD11b⁺/Ly6C^{med}/Ly6G⁺ myeloid cells represent the granulocytic subset of a heterogeneous class of myeloid cells termed myeloid-derived suppressor cells (MDSCs; ref. 16). The monocytic fraction (CD11b⁺/Ly6C^{high}/Ly6G⁻) suppresses CD8⁺ T cell and NK cell function, but the role of the granulocytic fraction is still unclear (16). It is described however, that the suppressive function of MDSCs is regulated by hypoxia,

Figure 2. The hypoxia-driven premetastatic niche is prometastatic. A, B16F10 metastatic foci in lungs of PyMT-WT NCM or HCM-treated mice counted by dissecting microscope 2 weeks after tumor cell injection (indicated by arrowheads in representative images; $n = 10/\text{group}$). Mean \pm SEM. B and C, cytokine (B) and angiogenesis (C) arrays were incubated with PyMT-WT or EO771 NCM and HCM. Factors increased (red boxes) or decreased (blue boxes) in HCM are listed in Supplementary Fig. S2B. D, flow cytometry analysis of lungs 4 weeks after Cherry-positive tumor cell injection and treatment with PyMT-WT NCM/HCM alone, or neutralized with MCP-1 antibody ($n = 4-5$). Mean percentage \pm SEM.



with Hif-1 α considered vital in controlling their differentiation into immunosuppressive macrophages (16).

We next determined whether CD11b⁺/Ly6C^{med}/Ly6G⁺ myeloid cells in the premetastatic niche controlled metastasis formation. As neutralization of MCP-1 in HCM decreased metastatic tumor burden (Fig. 2D), we assessed whether the myeloid cell composition of the premetastatic niche was also altered after MCP-1 neutralization. CD11b⁺/Ly6C^{med}/Ly6G⁺, but not CD11b⁺/Ly6C^{high}/Ly6G⁻ cells, were reduced when MCP-1 was neutralized in HCM but not NCM-treated mice (Supplementary Fig. S3A and B). Thus, accumulation of granulocytic CD11b⁺/Ly6C^{med}/Ly6G⁺ myeloid cells, driven by hypoxic tumor cell-derived MCP-1, regulates the premetastatic properties of the premetastatic niche.

NK cells in the premetastatic niche control metastasis formation

We next investigated other BMDC populations in the premetastatic niche. Although the abundance of CD8⁺ and CD4⁺ T cells, dendritic cells (CD11c⁺/MHC class II⁺), and macrophages (CD11b⁺/MHC class II⁺/F480⁺) was unchanged (Supplementary Fig. S4A), CD3⁻/NK1.1⁺ NK cells were enriched in lungs of HCM-treated mice (Fig. 3D). Characterization of these NK cells showed no difference in expression of the early activation marker CD69 (Supplementary Fig. S4B), whereas expression of the differentiation markers CD11b and CD27 (17) was significantly altered in the lungs of HCM-treated mice (Fig. 4A, left panel). The transition from CD11b^{low}/CD27^{low} to

CD11b^{high}/CD27^{low} defines immature and mature NK cells respectively, with a higher abundance of terminally differentiated mature CD11b^{high}/CD27^{low} NK cells found in the lung (17). We observed mature NK cells in lungs of untreated and NCM-treated mice (Fig. 4A, right panel), whereas HCM treatment resulted in reduced NK cell maturity (Fig. 4A, left panel), suggesting that HCM-derived factors hinder the differentiation of NK cells in the premetastatic niche. Comparing the cytotoxic effector capabilities of NK cells, HCM treatment resulted in lung NK cells with a markedly reduced capacity to kill YAC-1 target tumor cells (Fig. 4B). Therefore, although HCM-treated mice showed increased NK cell numbers in the premetastatic niche, these NK cells were overall less mature and poorly cytotoxic.

As effector lymphocytes of the innate immune system, NK cells are important in regulating metastasis, but have decreased cytotoxicity in both cancer patients and tumor-bearing mice (18). We hypothesized that the increase in metastasis observed in HCM-treated mice could be explained by the decreased ability of NK cells to eliminate incoming tumor cells and used 2 models of *in vivo* NK cell depletion to investigate this.

Rag2^{-/-}c. γ ^{-/-} mice, which lack B, T, and NK cells, were treated with NCM or HCM before injection with Cherry-positive PyMT-WT tumor cells. In contrast to immune-competent models (Fig. 1C and D), we found no difference in metastatic burden after NCM or HCM treatment (Fig. 4C). To investigate the effect of NK cells on metastasis formation in

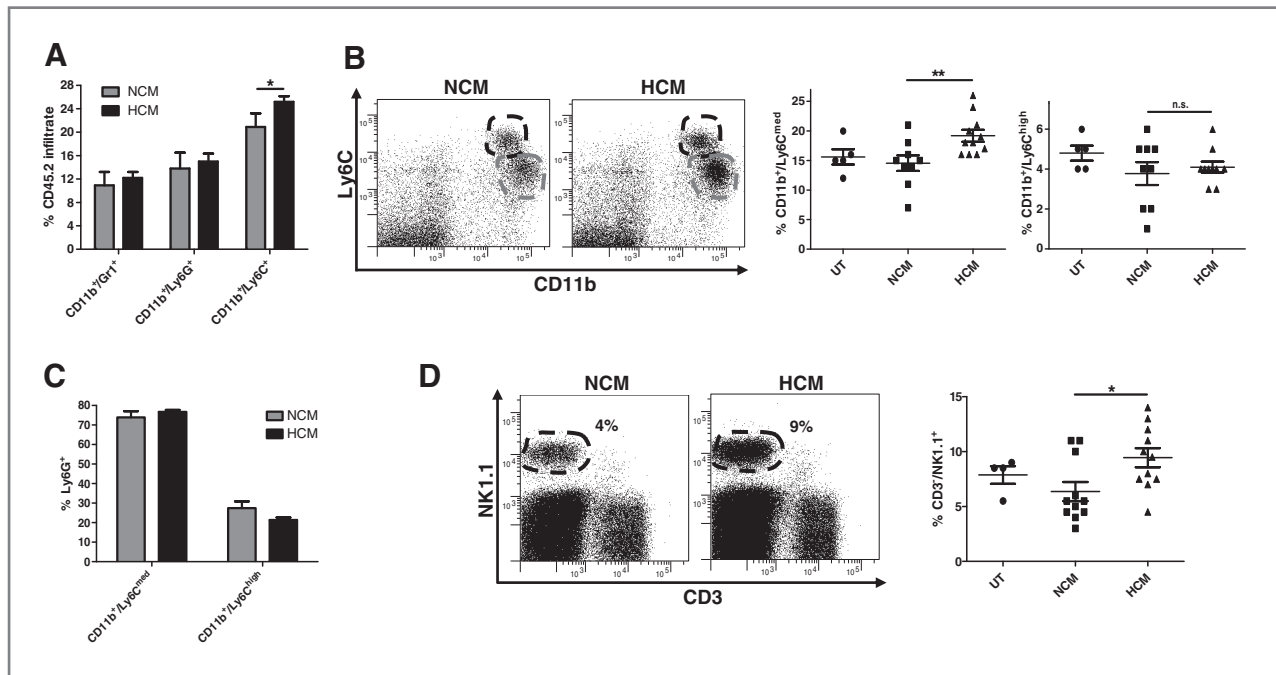


Figure 3. CD11b⁺/Ly6C^{med}/Ly6G⁺ and CD3⁻/NK1.1⁺ cells are increased in the lung under hypoxia. A, flow cytometry analysis of Gr-1, Ly6G, and Ly6C CD11b⁺ cell populations within eGFP⁺ BMDC lung infiltrate in PyMT-WT NCM- and HCM-treated mice (*n* = 10/group). B, representative flow cytometric plots of distinct CD11b⁺/Ly6C^{med} (gray line) and CD11b⁺/Ly6C^{high} (black line) subpopulations. Quantification of CD11b⁺/Ly6C^{med} (middle) and CD11b⁺/Ly6C^{high} (right) cells in lungs of UT (*n* = 5), PyMT-WT NCM, and HCM-treated mice (*n* = 11/group). C, Ly6G positivity in CD11b⁺/Ly6C^{med} and CD11b⁺/Ly6C^{high} subpopulations. D, representative flow cytometric plots for CD3⁻/NK1.1⁺ cells (circled) and total percentage in lungs from UT (*n* = 4), PyMT-WT NCM, and HCM-treated mice (*n* = 11/group). Mean percentage ± SEM.

immune-competent mice, we specifically depleted NK cells with anti-asialo-GM1 (Supplementary Fig. S4C). There was no significant change in tumor cells in the lungs of anti-asialo-

GM1/HCM compared with isotype/HCM-treated mice (Fig. 4D). In contrast, ablation of NK cells in anti-asialo-GM1/NCM-treated mice resulted in a significant increase in tumor cells

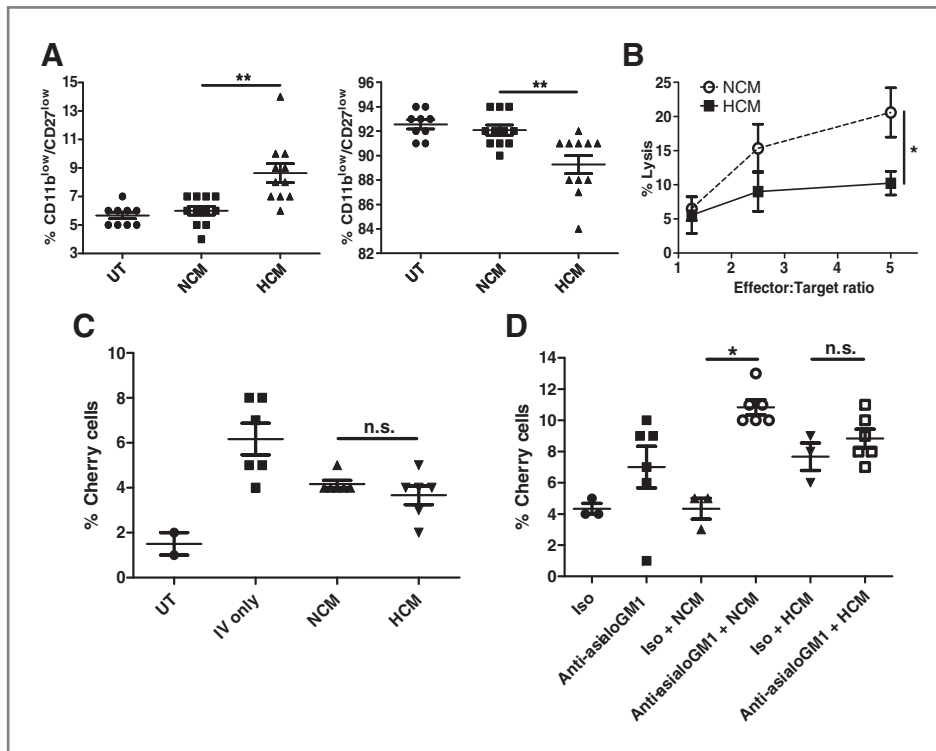


Figure 4. NK cell cytotoxicity is reduced in HCM-induced premetastatic niche. A, flow cytometry analysis of percent CD3⁻/NK1.1⁺ cells that are CD11b^{low}/CD27^{low} (left) or CD11b^{high}/CD27^{low} (right) from lungs of NCM and HCM-treated mice (UT *n* = 9/group; NCM/HCM *n* = 11/group). Mean percentage ± SEM. B, ⁵¹Cr release cytotoxicity assay for percent lysis of target YAC-1 cells by effector NK cells at indicated effector to target ratios (*n* = 3 independent experiments in duplicate). C and D, flow cytometry analysis for percent Cherry-positive PyMT-WT tumor cells in lungs 4 weeks after injection in C Rag2^{-/-}c.γ^{-/-} (*n* = 6/group) or mice treated with asialo-GM1 antibody (*n* = 6/group; D) or isotype (*n* = 3/group), and pretreated with PyMT-WT NCM or HCM. Mean percentage ± SEM.

compared with isotype/NCM-treated mice (Fig. 4D), suggesting that the lower metastatic burden in NCM-treated mice is mediated by antitumor activities of NK cells. Hence, molecules released by hypoxic primary tumor cells can reduce NK cell cytotoxic capacities, thus disabling the major innate antitumor response and creating a permissive niche for metastasis.

Our data showed that hypoxic mammary tumor cells secrete a variety of cytokines and growth factors, including MCP-1, to create a premetastatic niche populated by a specific subset of myeloid cells (CD11b⁺/Ly6C^{med}/Ly6G⁺). These findings suggest that the reduced antitumor activity of NK cells in the premetastatic niche may be attributed to the concomitant increase of CD11b⁺/Ly6C^{med}/Ly6G⁺ myeloid cells. In support of this, myeloid cell accumulation has been inversely correlated with suppression of NK cell function in a tumor-specific and contact-dependent manner in murine tumor models (18–20). The exact nature of this relationship in the premetastatic niche needs to be addressed in future studies. Our work uncovered, for the first time, that a population of NK cells with reduced cytotoxicity accumulate in the premetastatic niche, creating a microenvironment supporting metastatic growth of disseminated tumor cells.

Disclosure of Potential Conflicts of Interest

No potential conflicts of interest were disclosed.

References

1. Semenza GL. Defining the role of hypoxia-inducible factor 1 in cancer biology and therapeutics. *Oncogene* 2010;29:625–34.
2. Joyce JA, Pollard JW. Microenvironmental regulation of metastasis. *Nat Rev Cancer* 2009;9:239–52.
3. Wels J, Kaplan RN, Rafii S, Lyden D. Migratory neighbors and distant invaders: tumor-associated niche cells. *Genes Dev* 2008;22:559–74.
4. Eriqer JT, Bennewith KL, Cox TR, Lang G, Bird D, Koong A, et al. Hypoxia-induced lysyl oxidase is a critical mediator of bone marrow cell recruitment to form the premetastatic niche. *Cancer Cell* 2009;15:35–44.
5. Wong CC, Gilkes DM, Zhang H, Chen J, Wei H, Chaturvedi P, et al. Hypoxia-inducible factor 1 is a master regulator of breast cancer metastatic niche formation. *Proc Natl Acad Sci U S A* 2011;108:16369–74.
6. Kaplan RN, Riba RD, Zacharoulis S, Bramley AH, Vincent L, Costa C, et al. VEGFR1-positive haematopoietic bone marrow progenitors initiate the pre-metastatic niche. *Nature* 2005;438:820–7.
7. Psaila B, Lyden D. The metastatic niche: adapting the foreign soil. *Nat Rev Cancer* 2009;9:285–93.
8. Frew IJ, Hammond VE, Dickens RA, Quinn JM, Walkley CR, Sims NA, et al. Generation and analysis of Siah2 mutant mice. *Mol Cell Biol* 2003;23:9150–61.
9. Moller A, House CM, Wong CS, Scanlon DB, Liu MC, Ronai Z, et al. Inhibition of Siah ubiquitin ligase function. *Oncogene* 2009;28:289–96.
10. Chan CJ, Andrews DM, McLaughlin NM, Yagita H, Gilfillan S, Colonna M, et al. DNAM-1/CD155 interactions promote cytokine and NK cell-mediated suppression of poorly immunogenic melanoma metastases. *J Immunol* 2010;184:902–11.
11. Kaelin WG Jr, Ratcliffe PJ. Oxygen sensing by metazoans: the central role of the HIF hydroxylase pathway. *Mol Cell* 2008;30:393–402.
12. Kowanetz M, Wu X, Lee J, Tan M, Hagenbeek T, Qu X, et al. Granulocyte-colony stimulating factor promotes lung metastasis through mobilization of Ly6G+Ly6C+granulocytes. *Proc Natl Acad Sci U S A* 2010;107:21248–55.
13. Yan HH, Pickup M, Pang Y, Gorska AE, Li Z, Chytil A, et al. Gr-1+CD11b+ Myeloid cells tip the balance of immune protection to tumor promotion in the premetastatic lung. *Cancer Res* 2010;70:6139–49.
14. Castellani ML, Bhattacharya K, Tagen M, Kempuraj D, Perrella A, De Lutiis M, et al. Anti-chemokine therapy for inflammatory diseases. *Int J Immunopathol Pharmacol* 2007;20:447–53.
15. Gao D, Joshi N, Choi H, Ryu S, Hahn M, Catena R, et al. Myeloid progenitor cells in the premetastatic lung promote metastases by inducing mesenchymal to epithelial transition. *Cancer Res* 2012;72:1384–94.
16. Chioda M, Peranzoni E, Desantis G, Papalini F, Falisi E, Solito S, et al. Myeloid cell diversification and complexity: an old concept with new turns in oncology. *Cancer Metastasis Rev* 2011;30:27–43.
17. Hayakawa Y, Smyth MJ. CD27 dissects mature NK cells into two subsets with distinct responsiveness and migratory capacity. *J Immunol* 2006;176:1517–24.
18. Liu C, Yu S, Kappes J, Wang J, Grizzle WE, Zinn KR, et al. Expansion of spleen myeloid suppressor cells represses NK cell cytotoxicity in tumor-bearing host. *Blood* 2007;109:4336–42.
19. Li H, Han Y, Guo Q, Zhang M, Cao X. Cancer-expanded myeloid-derived suppressor cells induce anergy of NK cells through membrane-bound TGF-beta 1. *J Immunol* 2009;182:240–9.
20. Mauti LA, Le Bitoux MA, Baumer K, Stehle JC, Golshayan D, Provero P, et al. Myeloid-derived suppressor cells are implicated in regulating permissiveness for tumor metastasis during mouse gestation. *J Clin Invest* 2011;121:2794–807.

Authors' Contributions

Conception and design: B.S. Parker, D.D. Bowtell, M.J. Smyth, A. Möller
Development of methodology: J. Sceneay, A. Möller
Acquisition of data (provided animals, acquired and managed patients, provided facilities, etc.): J. Sceneay, A. Chen, H.M. Halse, C.S.F. Wong
Analysis and interpretation of data (e.g., statistical analysis, biostatistics, computational analysis): J. Sceneay, D.M. Andrews, E.K. Sloan, D.D. Bowtell, M. J. Smyth, A. Möller
Writing, review, and/or revision of the manuscript: J. Sceneay, M.T. Chow, C.S.F. Wong, D.M. Andrews, E.K. Sloan, B.S. Parker, D.D. Bowtell, M.J. Smyth, A. Möller
Administrative, technical, or material support (i.e., reporting or organizing data, constructing databases): M.T. Chow, B.S. Parker, D.D. Bowtell
Study supervision: M.J. Smyth, A. Möller

Acknowledgments

The authors thank Dr. Michele Teng for providing the Rag2^{-/-}cγ^{-/-} mice, Mira Liu for assistance with immunofluorescence, and Dr. Klaus Matthaei for providing the NZeg-eGFP mice.

Grant Support

The study was supported by Association of International Cancer Research project grant to A. Möller, State Trustees Australia Foundation scholarship to J. Sceneay, National Breast Cancer Foundation Fellowship to A. Möller and E.K. Sloan, National Health and Medical Research Council (NH&MRC) Australia Fellowship, NH&MRC Program Grant, and Victorian Cancer Agency support to M.J. Smyth, NH&MRC project grant to D.M. Andrews and E.K. Sloan, NHMRC CDA to B.S. Parker and D.M. Andrews, Cancer Research Institute Scholarship and Beaney Scholarship in Pathology to M.T. Chow, and NIH grant to E.K. Sloan.

Received November 30, 2011; revised April 16, 2012; accepted May 19, 2012; published OnlineFirst July 2, 2012.